The Glass Transition Temperature (T_g) as a Parameter for Monitoring the Cure of an Amine/Epoxy System at Constant Heating Rates

G. WISANRAKKIT, J. K. GILLHAM, and J. B. ENNS,* *Polymer Materials Program, Department of Chemical Engineering, Princeton University, Princeton, New Jersey 08544*

Synopsis

A continuous heating transformation (CHT) cure diagram displays the time and temperature of events that a material encounters during the course of continuous heating at different heating rates. For thermosetting systems, these events include gelation, vitrification, and devitrification. Analysis of isothermal data for a diglycidyl-type epoxy/tetrafunctional aliphatic amine system, which is initially liquid at room temperature, indicated that kinetic control applied prior to vitrification; i.e., for $T_g < T_{cure}$ (temperature of reaction). The parameters so obtained (i.e., order of reaction, Arrhenius pre-exponential term, and activation energy) together with an experimental relationship between T_g and extent of reaction were used as a basis for modeling the onset of vitrification and devitrification in the CHT diagram. For heating scans from below T_{go} (glass transition temperature of the reactants), initial devitrification occurs when T_{cure} first passes through the T_g of the initial reacting material, except for very low heating rates for which initial devitrification is not encountered. Vitrification is identified as the point at which T_g becomes equal to the increasing curing temperature. Diffusion control retards the reaction rate beyond vitrification. In the limiting case of complete retardation of the rate after vitrification, the reaction can proceed along the $T_g = T_{cure}$ path as long as the additional reaction with increasing temperature is sufficient to increase T_g at least at the same rate as the heating temperature; devitrification occurs thereafter. The critical heating rates at which the material does not devitrify in the vicinity of T_{go}, and that at which no vitrification is encountered, are calculated.

INTRODUCTION

The concept of the isothermal time-temperature-transformation (TTT) cure diagram (Fig. 1) is useful for understanding the behavior of thermosetting systems under isothermal cure conditions.[1,2] The diagram displays the times to reach certain events during isothermal cure vs. cure temperature. Events common to most liquid thermosetting polymers include gelation which corresponds to the incipient formation of an infinite network; vitrification, which occurs when the glass transition temperature (T_g) rises to the temperature of the cure reaction (T_{cure}); and devitrification, which occurs when T_g falls below

* Present address: Vistakon, Jacksonville, Florida 32216.

Journal of Applied Polymer Science, Vol. 41, 1895–1912 (1990)
 CCC 0021-8995/90/7-81895-18$04.00

T_{cure} due to degradation. Cure reactions proceed to some degree beyond vitrification causing the glass transition temperature to be higher than the cure temperature (i.e., $T_g > T_{cure}$).[3,4]

Analogous to the isothermal TTT diagram is the continuous heating transformation (CHT) cure diagram (Fig. 2) which displays the times and temperatures required to reach similar events during the course of continuous heating at constant heating rates.[5,6] For low heating rates above the initial glass transition temperature of the unreacted material (T_{go}), chemical reaction in the early stages can proceed such that the T_g of the material rises at a faster rate than the reaction temperature (T_{cure}). Vitrification occurs when T_g equals T_{cure}. After vitrification, the reaction rate is greatly diminished because diffusion control becomes more pronounced in the glass transition region.[5,7-9] However, immediately after vitrification, T_g increases at least at the same rate as the temperature. At high temperatures towards the maximum glass transition of the cured material ($T_{g\infty}$), the reaction rate is further reduced due to low concentration of the reactants at high conversion. Eventually, the cure temperature rises above T_g and devitrification occurs. The reaction can then proceed to completion ($T_g = T_{g\infty}$) in the rubbery state.

For high heating rates, the glass transition temperature of the material never reaches the cure temperature. Thus, the reaction can proceed to completion entirely in the rubbery state without encountering vitrification or devitrification.

When heating scans start well below T_{go}, the starting material is in the glassy state. For higher heating rates, the material will pass through initial devitrification when the temperature reaches T_{go} (to become a liquid). However, for lower heating rates, the reaction rate near T_{go} can be sufficient to keep T_g rising at least at the same rate as the heating temperature. In such cases, the material need not devitrify below $T_{g\infty}$.

The principal technique used for determining the glass transition temperature in this laboratory has been Torsional Braid Analysis (TBA).[5,10] T_g as measured in this technique corresponds to a state approximately halfway (but closer to the rubbery side of the transition region) between the rubbery and glassy states.[1,11] Thus, in a continuous heating situation after gelation and until vitrification (measured $T_g = T_{cure}$), the material is basically in the rubbery state and the reaction is predominantly kinetically controlled. Beyond vitrification, diffusion control dominates the reaction kinetics until the occurrence of devitrification.

This study is an attempt to model the behavior of an epoxy/amine system under such continuous heating conditions. Vitrification and devitrification points in the CHT diagram are quantitatively calculated using the kinetic parameters determined from isothermal conversion data. The calculated CHT diagram is compared with the published experimental data obtained from Torsional Braid Analysis.[5] A preliminary report has been published.[9]

RESULTS AND DISCUSSION

Isothermal Reaction Kinetics of an Amine-Cured Epoxy System

The chemical system used in this study was a stoichiometric mixture of a diglycidyl ether of bisphenol A (Epon 828, Shell Chemical Co.) with a tetra-

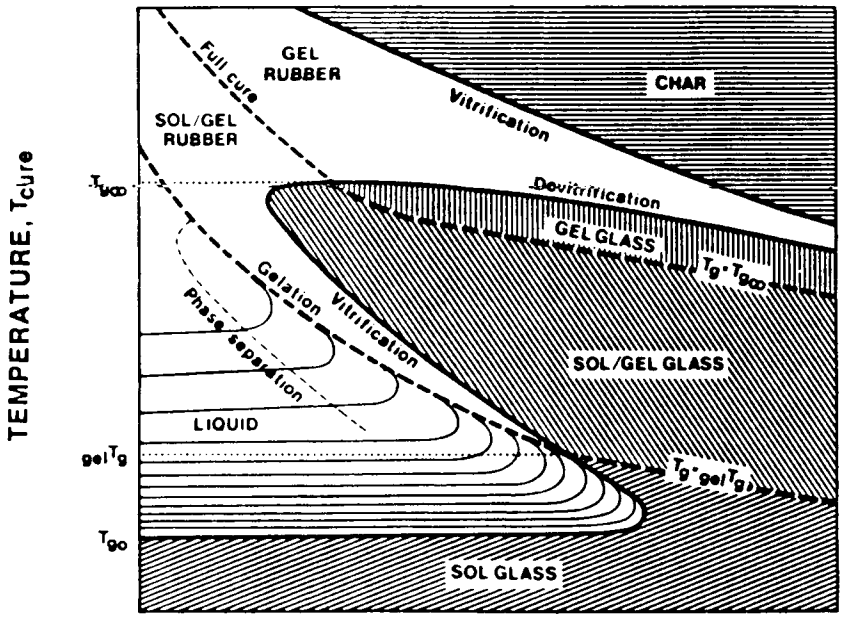

Fig. 1. Schematic time–temperature–transformation (TTT) isothermal cure diagram for a thermosetting system, showing three critical temperatures, i.e., $T_{g\infty,gel}T_g$, T_{go}, and the distinct states of matter, i.e., liquid, sol/gel rubber, gel rubber (elastomer), sol/gel glass, gel glass, sol (or ungelled) glass, and char. The full-cure line, i.e., $T_g = T_{g\infty}$, divides the gelled glass region into two parts: sol/gel glass and fully cured gel glass. (Phase separation, in two-phase systems, occurs prior to gelation. Successive isoviscous contours which are shown in the liquid region for a neat system with no phase separation differ by a factor of 10.) T_{go} is the initial glass transition temperature of the reactants; $_{gel}T_g$ is the glass transition temperature of the reaction system at its gelation point.

functional aliphatic amine, bis(p-aminocyclohexane) methane (PACM-20, DuPont). T_{go} and $T_{g\infty}$ for the mixture as determined by TBA are −19°C and 166°C, respectively.[2] The chemical structures of the two reactants are shown in Figure 3.

Conversion vs. time of isothermal curing data at different temperatures obtained using Fourier Transform Infrared (FTIR) spectroscopic analysis of the epoxy group absorption at 915 cm^{-1} are reproduced from Ref. 2 in Figure 4. Vitrification (from TBA) at each cure temperature is marked by an arrow. These data are reanalyzed in this report in order to obtain an expression which describes the chemical kinetics of the system under continuous heating conditions.

The rate of a chemically controlled reaction is given by the Arrhenius rate expression

$$\frac{dx}{dt} = kf(x) \tag{1}$$

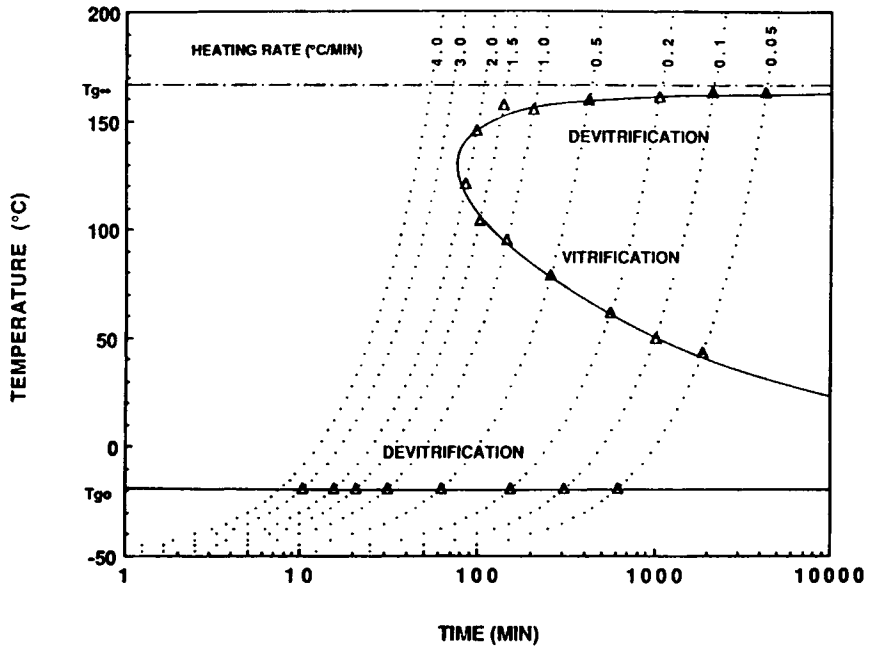

Fig. 2. Continuous heating transformation (CHT) cure diagram of EPON 828/PACM-20 which includes initial devitrification, vitrification, and devitrification events [from Ref. (5)].

where x = fractional conversion, k = Arrhenius rate constant = $A \exp(-E/RT)$ with A, E, and R having their usual significance, and T in absolute Kelvin. Rearranging, integrating and taking the natural logarithm of eq. (1) yields

$$F(x) = \ln\left[\int_0^x \frac{dx}{f(x)}\right] = \ln(k) + \ln(t) \tag{2}$$

REACTANTS

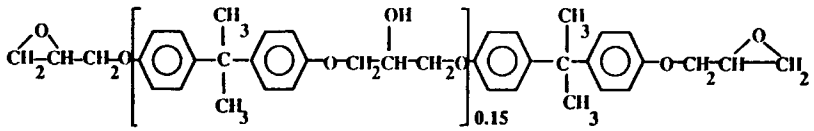

DIGLYCIDYL ETHER OF BISPHENOL A (EPON 828)

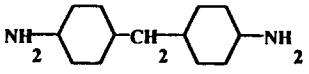

BIS(p-AMINOCYCLOHEXANE) METHANE (PACM-20)

Fig. 3. Chemical reactants.

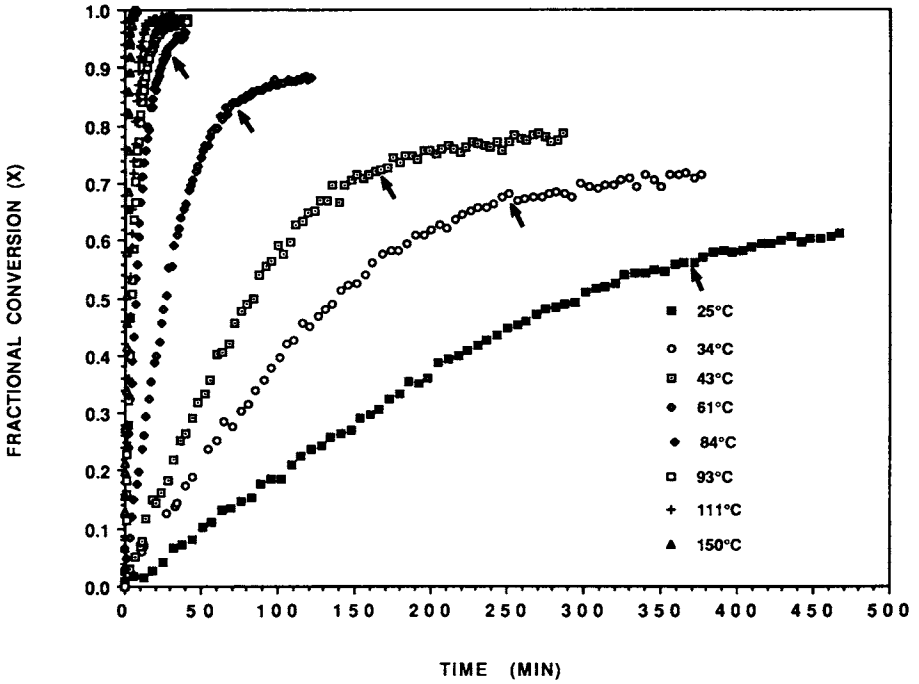

Fig. 4. Fractional conversion of epoxy vs. time during isothermal curing at different temperatures [FTIR results from Ref. (2)]. Experimental isothermal vitrification at each cure temperature is designated by an arrow.

Eq. (2) suggests that for kinetically controlled reaction, all isothermal x vs. ln(time) curves at different cure temperatures should be superimposable by simply shifting all curves horizontally relative to a curve at a fixed reference temperature.[12] The data in Figure 4 are replotted as fractional conversion vs. ln(time) in Figure 5. The resulting plots are then shifted horizontally along the ln(time) axis relative to the low conversion (unvitrified) data at 61°C so as to form a master curve at 61°C. All of the low conversion data can be superimposed as shown in Figure 6, except for the data at 111° and 150°C (not shown). At high temperatures, the reaction proceeds very rapidly (e.g., at 150°C full conversion was achieved in less than 10 min). Consequently, the greater experimental errors in specifying the short cure times at 111° and 150°C can account for the two plots at these temperatures not being satisfactorily superimposable with those at lower cure temperatures.

It can be clearly observed from Figure 6 that the data before isothermal vitrification (marked by arrows) can be superimposed to form a smooth master curve. This master curve represents the kinetically controlled reaction as is implied by eq. (1). The data after vitrification at all lower cure temperatures ($T_{cure} \leq 61°C$) start to deviate from the master curve because the reaction becomes diffusion-controlled due to low segmental mobility. However, the similar effect of vitrification is not apparent for $T_{cure} = 84$ and 93°C (vitrification occurring at $x = 0.92$ and 0.94, respectively); the reason is that vitrification in these cases occurs at very high conversions, and small differences in the fractional conversion data are not easily distinguished. It has been demonstrated

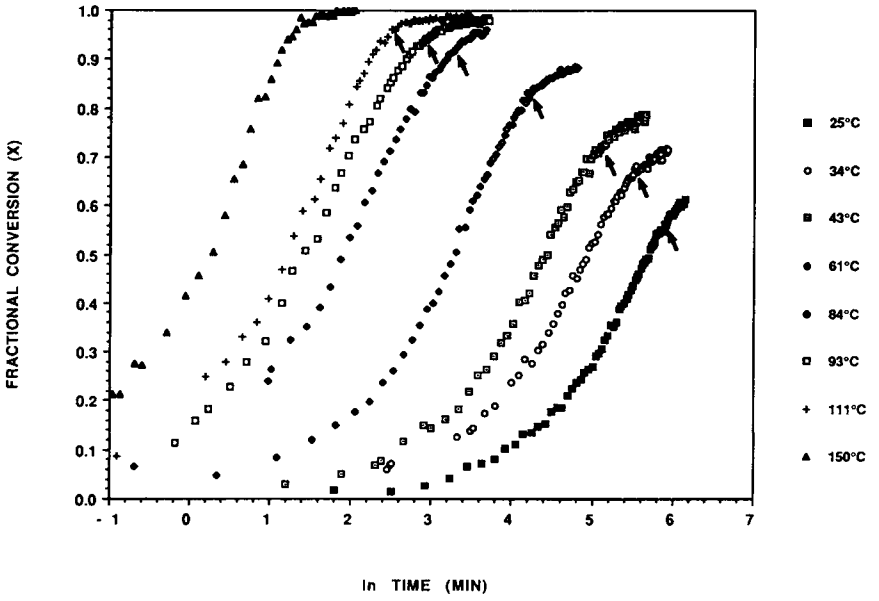

Fig. 5. Fractional conversion of epoxy vs. ln(time) at different cure temperatures (same data as in Fig. 4). Experimental isothermal vitrification at each cure temperature is designated by an arrow.

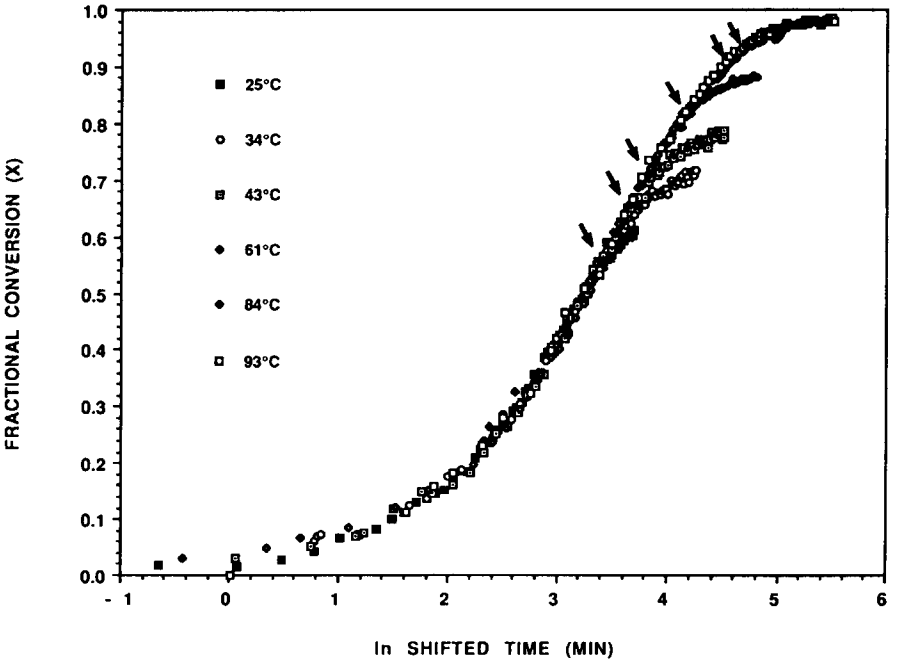

Fig. 6. Superposition of the conversion vs. ln(time) curves in Figure 5 (excluding the two plots at 111° and 150°C) by shifting all plots horizontally relative to the low conversion data at 61°C so as to form a kinetically controlled master curve at 61°C.

in our recent report[12] that the differences are more discernible when T_g is employed instead of fractional conversion, since a small change in conversion, especially at high conversion, is amplified in the corresponding change in T_g. The data of the composite master curve up to 94% conversion (i.e., kinetically controlled data prior to vitrification at all cure temperatures) are analyzed for the reaction kinetics in the following section.

The shift factor, A_T, is defined as the ln(time) difference at constant conversion between curves for different cure temperatures

$$A_T = \ln(t_1) - \ln(t_2) = \ln(k_2) - \ln(k_1) = -\frac{E}{R}\left(\frac{1}{T_2} - \frac{1}{T_1}\right) \tag{3}$$

The shift factors used in shifting all of the curves relative to 61°C (for constructing the master curve in Fig. 6) are summarized in Table I.

For reaction with a single apparent activation energy, E, eq. (3) states that plotting the shift factor against the corresponding reciprocal cure temperature should yield a straight line with slope equal to $-E/R$. Figure 7 shows a plot of the shift factors in Table I vs. $1/T$. The results can be correlated with a straight line, the slope of which yields an apparent activation energy of 13.3 Kcal/mol.

The kinetically controlled master curve (in Fig. 6) is analyzed for this report with an ordinary nth-order kinetic rate expression, eq. (4). It is assumed that the only reaction occurring is that between one epoxy and one amino hydrogen, and that primary and secondary amino hydrogens react with epoxy with equal reactivity.

$$\frac{dx}{dt} = k(1 - x)^n \tag{4}$$

A previous study[2] suggests that the isothermal reaction kinetics of this epoxy/amine system can be adequately described by a first-order rate expression [eq. (4) with $n = 1$]. Plotting dx/dt vs. $(1 - x)$ of the kinetically controlled master curve data results in a straight line, the slope of which yields the value of the rate constant at 61°C equal to 0.0262 min^{-1} as shown in Figure 8. The first order calculation of x vs. t using the determined value of k at 61°C is shown as

TABLE I
Shift Factors Relative to 61°C for Different Cure Temperatures

T_{cure} (°C)	Shift factor [$A_T = \ln(t_{61°C}) - \ln(t_T)$]
25	−2.444
34	−1.676
43	−1.149
61	0.000
84	1.352
93	1.800

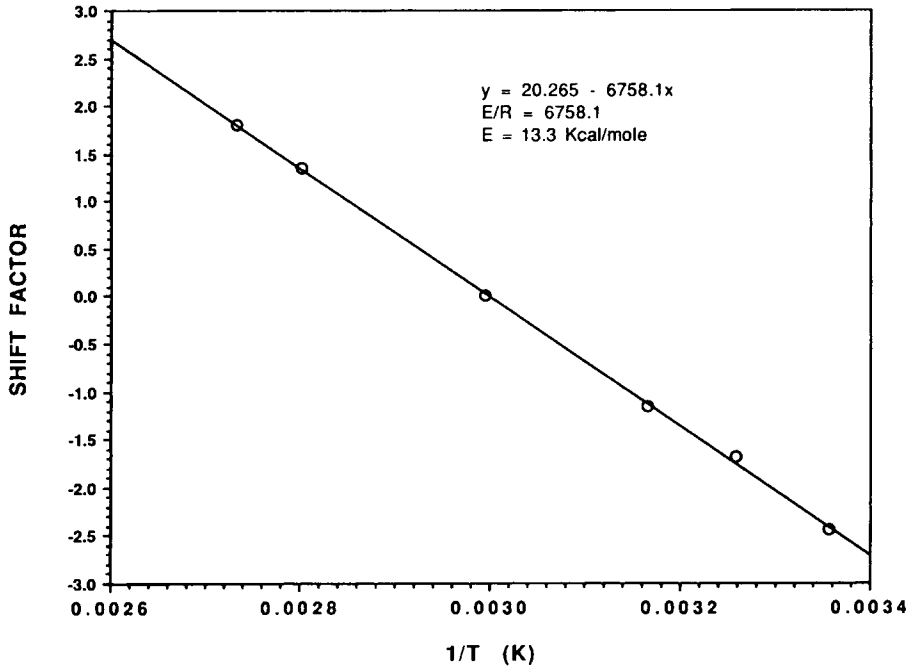

Fig. 7. Arrhenius plot of the shift factors, $[A_T = \ln(t_{61°C}) - \ln(t_T)]$, which were used in constructing the master curve in Figure 6, vs. $1/T(K)$. The activation energy for the reaction is determined from the slope of the straight line.

a solid curve in Figure 9. The calculation appears to correlate well with the experimental data (circles) up to 94% conversion.

There is ample evidence in the literature, however, which shows the kinetics of the reation between different epoxy and amine systems to be second order autocatalyzed by hydroxyl groups generated during the reaction.[13-19] Assuming equal reactivities of all amino hydrogens, which is generally found to be applicable for aliphatic amine/epoxy systems,[20,21] the reaction rate for a stoichiometric mixture of epoxy and amine can be expressed on a fractional conversion basis[22] as

$$\frac{dx}{dt} = k(1 - x)^2(x + B) \tag{5}$$

where B is a constant related to the initial concentration of impurities which act as catalysts to accelerate the reaction.

The present data of the master curve are also analyzed according to the autocatalytic rate expression, eq. (5). Figure 10 shows a plot of $(dx/dt)/(1 - x)^2$ vs. x. The results up to approximately 60% conversion can be correlated with a straight line, the slope and intercept of which give the values for k and kB equal to 0.0857 min^{-1} and 0.0175, respectively. Using the values of k and B, eq. (5) can be solved numerically by the Runge-Kutta integration technique[23] to yield conversion as a function of time. The results of the numerical integration are shown as a solid curve in Figure 11. The calculation appears to agree with

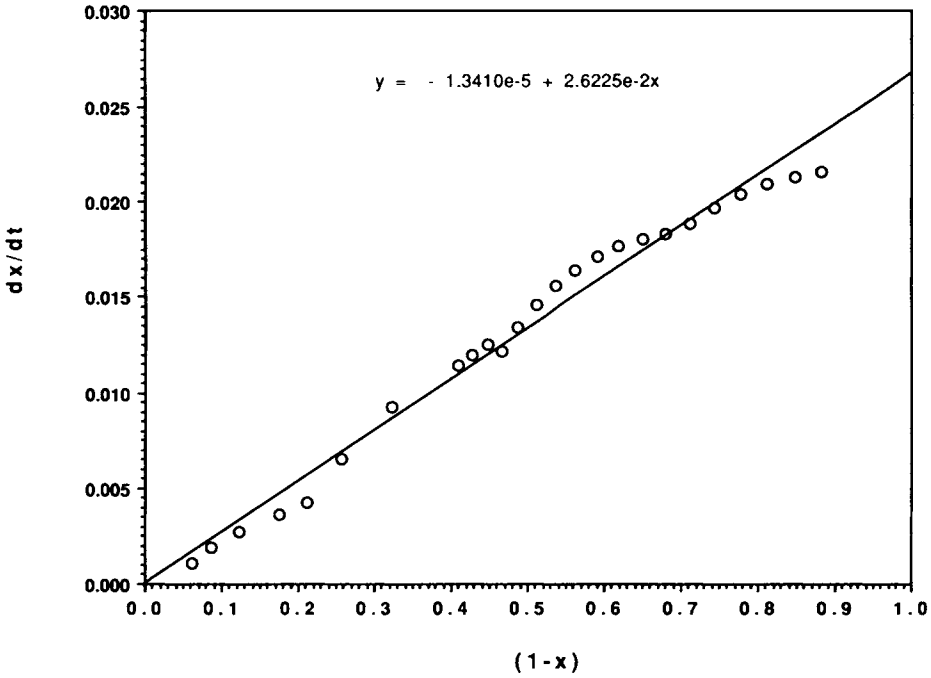

Fig. 8. Data of the master curve analyzed according to a first-order kinetic rate expression, $[dx/dt = k(1 - x)]$. The slope of the straight line yields the value of k at 61°C.

the experimental data up to 75% conversion. At higher conversions, the autocatalytic rate expression predicts lower conversions (up to approximately 4%) than the experimental data.

The parameters for both the first-order and the autocatalyzed reaction kinetics are summarized in Table II. Both kinetic rate expressions will be applied in the following section to model the onset of vitrification and devitrification under continuous heating at constant rates. The calculated results will be compared with experimental data obtained independently by the dynamic mechanical TBA technique, which can be a means to check the validity of each kinetic assumption.

The time to vitrify for isothermal cure versus temperature can be computed by calculating the time for the T_g to rise from its initial value to the temperature of reaction[2,24-26] (results for the present system not shown here). Experimental times to vitrify (determined by TBA technique) are marked on the plots of isothermal data in Figures 4, 5, and 6.

CHT Diagram

The dynamic mechanical behavior of the material during the course of continuous heating at a constant rate displays changes when the material encounters various events similar to those observed in the isothermal case. These events can include the initial glass to liquid transition, gelation, vitrification, and devitrification. Figure 12A shows the TBA relative rigidity of the material during continuous heating from below T_{go} to above $T_{g\infty}$ at different heating rates. The corresponding TBA logarithmic decrement data are shown in Figure

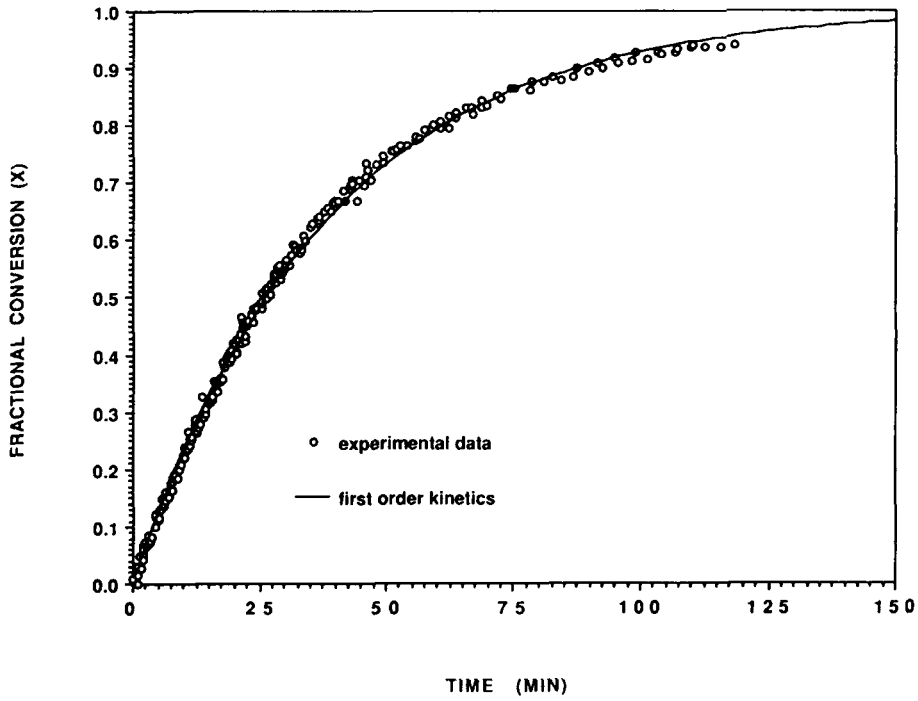

Fig. 9. Comparison of the calculation using first-order kinetics at 61°C (—) with the experimental master curve (○).

12B. Data are reproduced from Ref. (5). The initial devitrification (the first glass transition encountered during temperature scanning), vitrification, and devitrification near $T_{g\infty}$, were identified, respectively, from the maxima of the first, fourth, and fifth peaks (in the order of increasing temperature) in the logarithmic decrement spectra. The results are summarized in the form of a CHT diagram shown in Figure 2.[5] (Gelation will not be discussed in this report.)

Initial Devitrification and Vitrification Calculation

The initial devitrification and vitrification points at various heating rates in the CHT diagram can be calculated from knowledge of the reaction kinetics and the relationship between the glass transition temperature and the extent of reaction. At a given constant heating rate, c, $T_{\text{cure}} = T_i + ct$, where $T_i = 223$ K (−50°C) is the starting temperature. Assuming that the reaction is also kinetically controlled even for T_{cure} less than initial devitrification (i.e., the fastest case), the rate eq. (1) becomes

$$\frac{dx}{dt} = A \exp\left(\frac{-E}{R(T_i + ct)}\right) f(x) \tag{6}$$

If E, A, and the form of $f(x)$ have been determined, the rate equation can be integrated numerically to give x as a function of time.

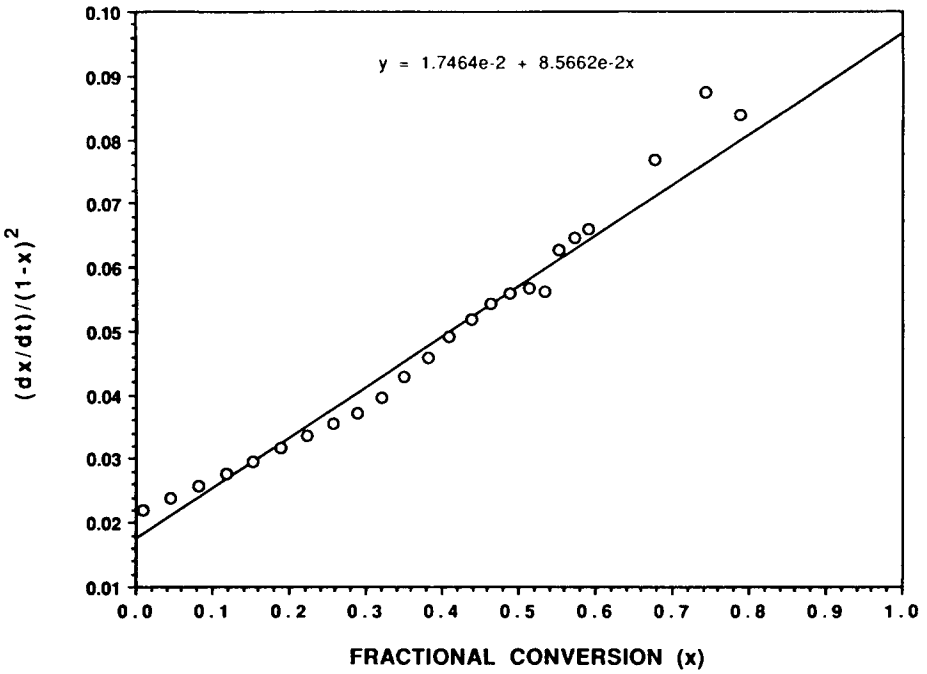

Fig. 10. Data of the master curve analyzed according to an autocatalyzed reaction kinetic rate expression, $[dx/dt = k(1 - x)^2(x + B)]$. The slope and intercept of the straight line yield the values for k and kB at 61°C, respectively.

An empirical relationship between T_g and x is given by the DiBenedetto relation[27] adapted in the manner of Adabbo and Williams[26]

$$\frac{T_g - T_{go}}{T_{go}} = \frac{(C_1 - C_2)x}{1 - (1 - C_2)x} \tag{7}$$

where C_1 and C_2 are constant parameters. This relationship implies a unique relationship between T_g and conversion. For the epoxy-amine system in this study, C_1 and C_2 were determined to be 0.335 and 0.194 respectively.[2] Employing this relation, T_g can be calculated for each conversion x. Eq. (6) together with eq. (7) govern how the T_g of the material increases as a function of time.

For a heating rate starting from below T_{go}, the initial devitrification is encountered when the cure temperature passes through the T_g of the reacting material. This event generally occurs at T_{go} at reasonably high heating rates. However, at very low heating rates, it can occur at $T_{\text{cure}} > T_{go}$, because the long time required for the temperature to reach T_{go} in these cases permits substantial chemical conversion which raises T_g above T_{go}; consequently, the material does not devitrify at T_{go}. The initial devitrification points at different heating rates constitute the initial devitrification curve (i.e., the lower section of the S-shaped initial devitrification–vitrification–upper devitrification envelope) in the CHT diagram.

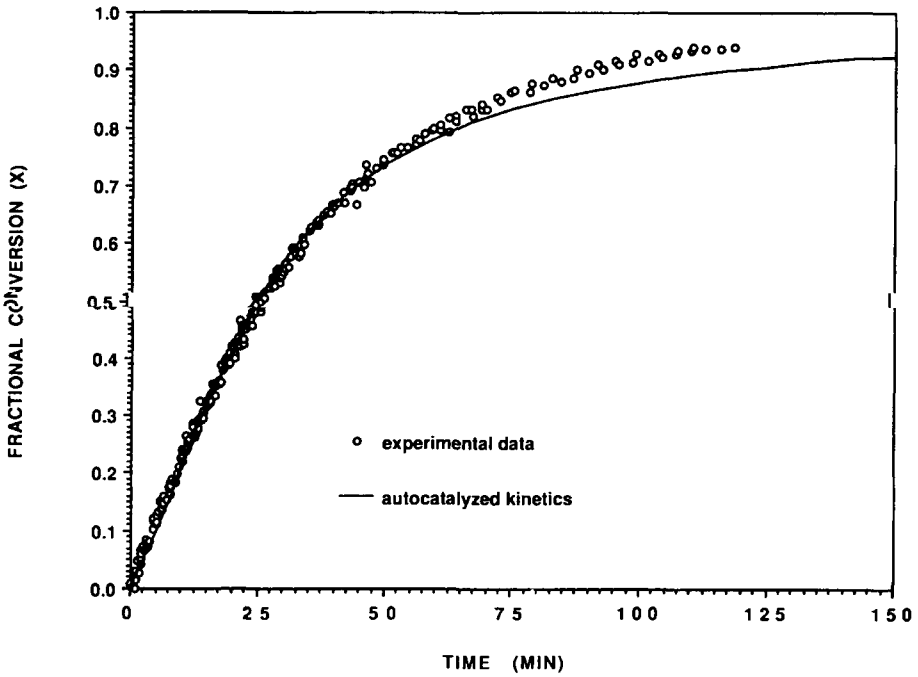

Fig. 11. Comparison of the calculation using autocatalyzed reaction kinetics at 61°C (—) with the experimental master curve (○).

After initial devitrification, the time and temperature at which T_g becomes equal to the increasing curing temperature is identified as a vitrification point. These points at different heating rates make up the vitrification curve (the middle section of the S-shaped enveloped) in the CHT diagram.

Upper Devitrification Calculation

Beyond the vitrification point in the CHT diagram, the material is in the glass transition region and the reaction of the system is affected by diffusion control. In the simplest limiting case, the reaction can proceed along the $T_g = T_{cure}$ path[15], i.e., T_g can follow the curing temperature as long as the additional conversion with each small temperature increment is sufficient to increase T_g to T_{cure}. However, eventually because of the high conversion at high temperature

TABLE II
Kinetic Parameters [Activation Energy (E), Arrhenius Pre-exponential Factor (A)] and the Form of $f(x)$ for the Assumed First-Order and Autocatalytic Kinetics

	First-order	Autocatalytic
E (Kcal/mol)	13.30	13.30
A (min^{-1})	1.34×10^7	4.36×10^7
$f(x)$	$(1 - x)$	$(1 - x)^2(x + 0.2038)$

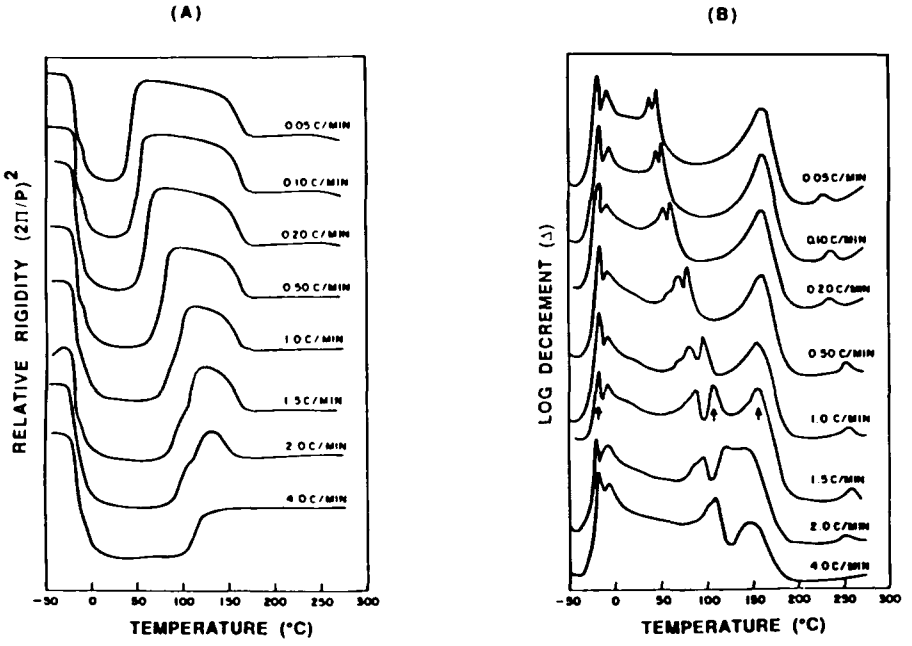

Fig. 12. TBA dynamic mechanical behavior of EPON 828/PACM-20 during continuous heating from below T_{g0} to above $T_{g\infty}$ at different rates: (**A**) relative rigidity and (**B**) logarithmic decrement [from Ref. (5)]. The events relevant to this work are the times to reach T_{g0}, vitrification and devitrification which are identified by the first, fourth and fifth peaks, respectively, in the logarithmic decrement in the order of increasing temperature (see, for example, the marked spectrum at 1.5°C/min). These events are summarized in the CHT diagram in Figure 2.

towards $T_{g\infty}$ or because of the relatively high rate of increase of temperature, the reaction rate is not sufficient to keep $T_g = T_{\text{cure}}$ and so devitrification occurs.

In order to quantitatively calculate the time to reach the devitrification temperature for a given heating rate, consider the time rate of change of T_g by chemical reaction which is given by

$$\frac{dT_g}{dt} = \left(\frac{dT_g}{dx}\right)\left(\frac{dx}{dt}\right) \tag{8}$$

The first term on the right hand side, dT_g/dx, is the rate of change of T_g with respect to conversion. This term can be derived from the DiBenedetto relationship, i.e.,

$$\frac{dT_g}{dx} = \frac{T_{g0}(C_1 - C_2)}{[1 - (1 - C_2)x]^2} \tag{9}$$

The second term, dx/dt, is the rate of chemical reaction which can be calculated from the assumed reaction kinetics [eq. (6)].

When dT_g/dt is greater than the heating rate, c, the chemical conversion is sufficient to keep T_g at the reaction temperature. Eventually, the reaction rate decreases, and dT_g/dt falls below the heating rate, resulting in devitrification. Devitrification is identified in the calculation as the point at which dT_g/dt equals the heating rate. The locus of this devitrification process at different

heating rates constitutes the upper devitrification curve in the CHT diagram.

The calculation scheme to determine the devitrification point is as follows:

1. At the vitrification point, calculate the conversion, x, corresponding to T_g using the T_g vs. x relationship, eq. (7).
2. For a small time increment from the vitrification point, determine the cure temperature from the heating rate (i.e., $T_{cure} = T_i + ct$)
3. Assuming that the reaction remains kinetically controlled, calculate dx/dt from the assumed kinetic rate law [eq. (6)] and dT_g/dx from eq. (9).
4. Evaluate dT_g/dt from eq. (8).
5. If dT_g/dt is greater than the heating rate, the additional reaction in this time increment is sufficient to keep $T_g = T_{cure}$. Calculate the conversion corresponding to this new T_g.
6. Repeat steps 2 to 5 for the next small time increment until the devitrification point is reached (i.e., the point at which dT_g/dt starts to fall below the heating rate).

It should be emphasized that the above procedure is only a limiting case since it assumes that the reaction proceeds along the $T_g = T_{cure}$ path after vitrification. It is apparent from the isothermal conversion data in Figure 6 that the reaction can proceed significantly in the glass transition region ($T_g > T_{cure}$), although its rate decreases markedly due to diffusion control. In the actual continuous heating situation, the nonzero reaction rate after vitrification can keep T_g higher than T_{cure}. Therefore, the actual devitrification point can be a few degrees higher than the computed devitrification temperature. A more realistic model for the material behavior after vitrification must take into account the fact that T_g can be higher than T_{cure} and can remain higher until devitrification. However, this requires knowledge of the diffusion controlled kinetics in the glass transition region, which is a subject under current investigation.[28]

Calculation Results

Initial Devitrification–Vitrification–Devitrification Envelope. The initial devitrification, vitrification and upper devitrification points were calculated at different heating rates for the two assumed kinetic rate equations using the kinetic parameters determined previously for each case (Table II). The results are shown as solid curves in the form of the CHT diagram in Figure 13 and Figure 14 for first-order and autocatalyzed reaction kinetics, respectively. The calculations are compared with the experimental data (symbols) of the CHT diagram from Figure 2. It is apparent that autocatalyzed reaction kinetics give a better fit.

Although the autocatalytic model fits the isothermal data to only 75% conversion, whereas the first-order kinetics fits to 94%, both can still be considered reasonable representations due to the decreasing accuracy of the measurement of conversion with increasing conversion. However, in view of the better fit of the data under continuous heating conditions using the autocatalytic model, it is considered to be a better representation of the kinetics of the overall cure process.

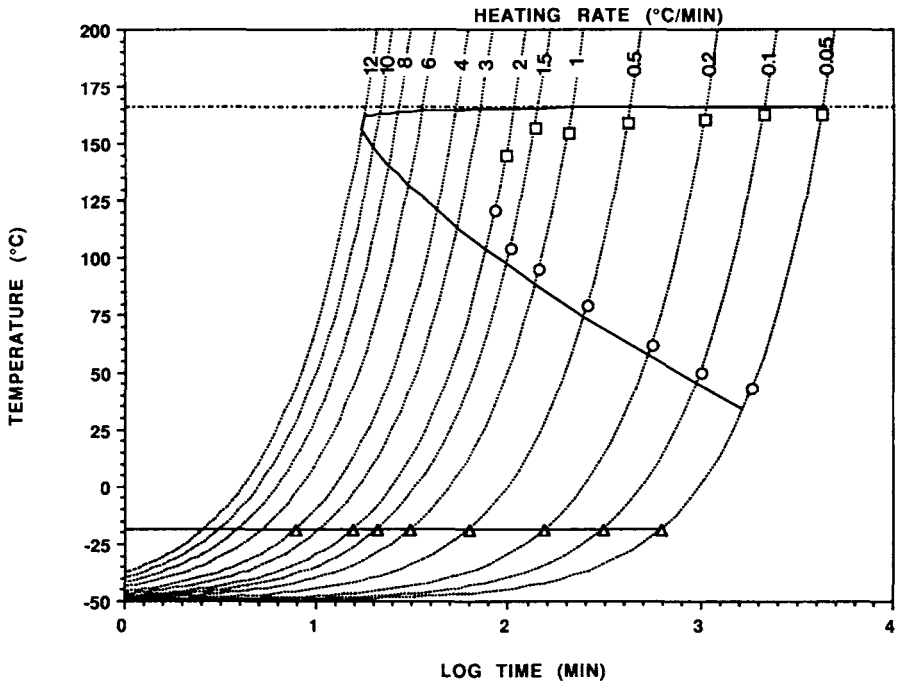

Fig. 13. Calculated CHT (vitrification and upper devitrification) diagram from first order kinetics (solid curves), also included: experimental data (symbols) (from Fig. 2).

Limiting Heating Rates. It can be noted from the calculation in Figure 14 (for the case with autocatalyzed reaction kinetics) that there are two critical heating rates: the lower limiting heating rate, c_L, at which initial devitrification and vitrification occur simultaneously, and the higher limiting heating rate, c_H, at which vitrification and upper devitrification occur simultaneously.

Assuming the fastest case in which the reaction is kinetically controlled for $T_{\text{cure}} \geq -50°\text{C}$, the low limiting heating rate for the present system is determined to be 4.13×10^{-3} °C/min. For heating rates less than this value, the material does not devitrify until the temperature is close to or at $T_{g\infty}$, since the reaction can raise T_g at least at the same rate as the cure temperature. In these cases, the system will polymerize without liquifying; i.e., polymerization occurs under conditions of maximum density. It is anticipated that such a cure process of heating to just short of $T_{g\infty}$ can produce material with less internal stresses, since no change in state is encountered during cure.

A dashed S-shaped contour included in Figure 14 represents the CHT envelope which would result assuming that the reaction does not commence until the temperature reaches T_{go} (i.e., the slowest case with no reaction below T_{go}). In such a case, the low limiting heating rate without initial devitrification would be 1.1×10^{-3} °C/min. The real low limiting heating rate will be between 1.1×10^{-3} and 4.13×10^{-3} °C/min, since in an actual situation, some reaction will proceed below T_{go} but will be under some influence of diffusion control in the glass transition region (i.e., actual reaction rate < kinetically controlled rate).

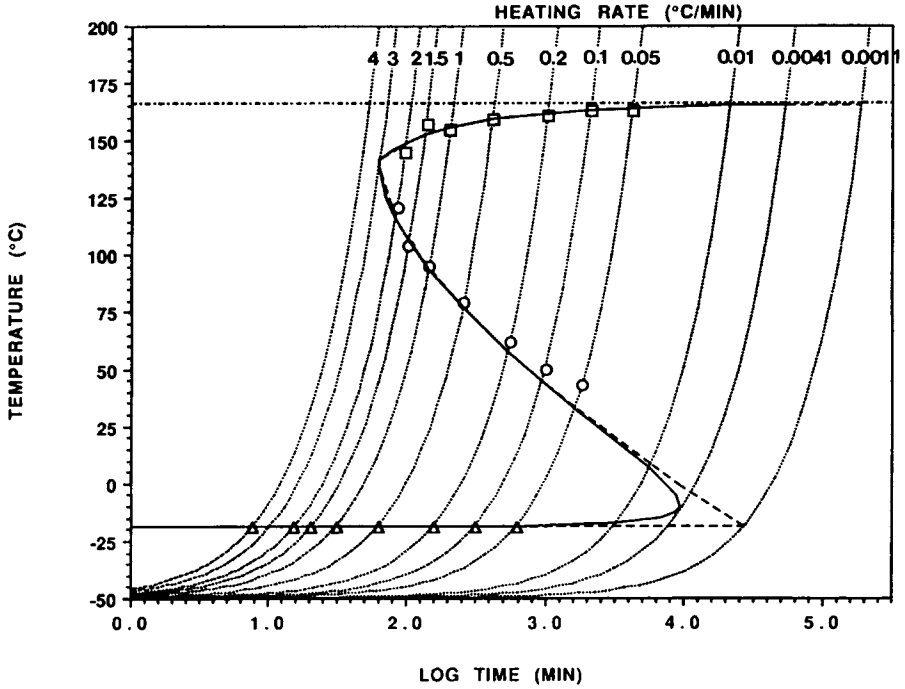

Fig. 14. Calculated CHT (initial devitrification, vitrification, and upper devitrification) diagram from autocatalyzed reaction kinetics: (—) assuming kinetic control for $T > -50°C$, (---) assuming no reaction proceeding below T_{go}. Experimental data (from Fig. 2): initial devitrification (Δ), vitrification (○), and upper devitrification near $T_{g\infty}$ (□). Note the critical heating rates: 3.03°C/min is the maximum heating rate that the material will encounter vitrification, and 4.13×10^{-3}°C/min is the minimum heating rate that the material will encounter initial devitrification.

Analogous to the low limiting heating rate without initial devitrification is the high limiting heating rate at which the material will not encounter vitrification during a temperature scan. This can be determined by calculating the heating rate, c_H, at which vitrification ($T_g = T_{\text{cure}}$) and devitrification ($dT_g/dt = c_H$) occur simultaneously.

Let t_v and x_v be the time and conversion to reach vitrification for the limiting heating rate c_H. The vitrification condition combined with DiBenedetto's relation can be expressed in terms of t_v, x_v, and c_H as

$$T_g = T_{go} + \frac{T_{go}(C_1 - C_2)x_v}{1 - (1 - C_2)x_v} = T_i + c_H t_v \tag{11}$$

The devitrification condition becomes

$$\left.\frac{dT_g}{dt}\right|_{vit} = \frac{T_{go}(C_1 - C_2)}{[1 - (1 - C_2)x_v]^2} A \exp\left(-\frac{E}{R(T_i + c_L t_v)}\right) f(x_v) = c_H \tag{12}$$

These two equations together with the rate expression, eq. (6), can be solved simultaneously for the three unknowns t_v, x_v, and c_H.

The calculations were performed numerically for the case of autocatalyzed reaction kinetics. The procedure assumes the heating rate, c_H, then calculates the time (t_v) and conversion (x_v) to reach vitrification for the assumed heating

rate. The time rate of change of T_g is then evaluated at the calculated vitrification point according to eq. (12). If dT_g/dt is greater than the heating rate c_H, the procedure is repeated for a new higher heating rate. If no vitrification is encountered, the guessed value of c_H is higher than the actual limiting heating rate. This trial and error procedure is repeated until the limiting heating rate is found. For autocatalyzed reaction kinetics, this value is found to be 3.03°C/min. Thus, for any heating rate greater than 3.03°C/min, the material will not encounter vitrification during the temperature scan.

This critical heating rate (c_H) has practical implications in molding technology. For example, it defines the minimum heating rate so as to obtain full conversion without the interference of vitrification. Conversely, vitrification can be an essential part of a cure cycle in order to control the reaction rates of highly exothermic reactions. The polymerization of more than 1 ton of epoxy to encapsulate a magnetic coil in Princeton University's experimental Tokomak nuclear fusion reactor is accomplished by heating at a very low rate of temperature increase ($\sim 7 \times 10^{-3}$°C/min); the reaction rate is controlled in the process by the T_g increasing in concert with the temperature until $T_{g\infty}$, i.e., full cure, is attained.[1]

CONCLUSIONS

1. Analyses of isothermal IR conversion data for this aliphatic amine/aromatic epoxy system show that there is a single apparent activation energy for the reaction as is evident from the superposition of the low conversion data vs. ln(time) curves at different cure temperatures forming a kinetically controlled master curve for isothermal reaction. The apparent activation energy for the reaction is 13.3 Kcal/mol. Perturbations of the data from the master curve occur after vitrification.
2. The isothermal chemical kinetics of the reaction can be equally well represented (up to 75% conversion) by a first-order and an autocatalytic rate expression. However, only the autocatalyzed reaction kinetics correctly describes the behavior of the system under continuous heating conditions. The CHT vitrification/devitrification envelope for this system is calculated using the autocatalytic kinetic parameters. The results agree quantitatively with the experimental vitrification/devitrification data which were independently obtained by the dynamic mechanical TBA technique.
3. Initially, in a continuous heating case, when the heating temperature passes through T_{go}, the unreacted glassy material will devitrify. For very low heating rates, however, no initial devitrification will be encountered since the reaction rate at T_{go} is sufficient to increase T_g at the same rate as the temperature. For autocatalyzed reaction kinetics, the minimum heating rate at which the material will devitrify at T_{go} is between 1.1×10^{-3} and 4.13×10^{-3}°C/min.
4. After initial devitrification, the reaction proceeds in the liquid and rubbery states during the temperature scans; vitrification is subsequently identified as the point at which T_g becomes equal to T_{cure}. After vitrifi-

cation, the upper devitrification envelope was computed by comparing the rate of change of T_g with respect to time, dT_g/dt, with the heating rate dT/dt assuming that the reaction proceeds along the $T_g = T_{cure}$ path, as long as the former is greater. The upper devitrification point is identified as the point at which dT_g/dt starts to fall below the heating rate (due to low reaction rate at high conversion, or because of a relatively high heating rate).

For autocatalyzed reaction kinetics, the critical heating rate at which vitrification and devitrification occur simultaneously is computed to be 3.03°C/min.

This research was supported in part by the Office of Naval Research.

References

1. J. K. Gillham, *Polym. Eng. Sci.*, **19**, 670 (1979). Ibid., **26**(20), 1429–1433 (1986).
2. J. B. Enns and J. K. Gillham, *J. Appl. Polym. Sci.*, **28**, 2567–2591 (1983).
3. X. Peng and J. K. Gillham, *J. Appl. Polym. Sci.*, **30**, 4685 (1985).
4. G. Palmese and J. K. Gillham, *J. Appl. Polym. Sci.*, **34**, 1925–1939 (1987).
5. J. B. Enns and J. K. Gillham, in American Chemistry Society Advances in Chemistry Series No. 203, *Polymer Characterization*, C. D. Craver, Ed., 27–63 (1983).
6. A. F. Lewis, M. J. Doyle, and J. K. Gillham, *Polym. Eng. Sci.*, **10**, 683 (1979).
7. I. Mita and K. Horie, *J. Macromol. Sci. Rev. Macromol. Chem. Phys.* C**27**(1), 91, (1987).
8. I. Havlicek and K. Dusek, in *Crosslinked Epoxies*, B. Sedlacek and J. Kahovec, Eds., 417, Walter de Gruyter, New York (1987).
9. G. Wisanrakkit, J. K. Gillham, and J. B. Enns, *Amer. Chem. Soc. Preprints Div. Polym. Mat. Sci. Eng.*, **57**, 87 (1987).
10. J. K. Gillham, in *Developments in Polymer Characterisation-3*, J. V. Dawkins, Ed., Applied Science Publishers, London, 1982, 159–227.
11. K. P. Pang and J. K. Gillham, *J. Appl. Polym. Sci.*, **37**, 1969–1999 (1989).
12. G. Wisanrakkit and J. K. Gillham, *J. Coat. Tech.*, **62**(783), 35–50 (1990).
13. K. Horie, H. Hiura, M. Sawada, I. Mita, and H. Kambe, *J. Polym. Sci.*, **8**, 1357 (1970).
14. S. Lunak and K. Dusek, *J. Polym. Sci. Polym. Symp.*, **53**, 45 (1976).
15. S. Lunak, J. Vladyka, and K. Dusek, *Polymer*, **19**, 931 (1978).
16. S. Sourour and M. R. Kamal, *Thermochim. Acta.*, **14**, 41 (1976).
17. A. Dutta and M. E. Ryan, *J. Appl. Polym. Sci.*, **24**, 635–649 (1979).
18. C. C. Riccardi, H. E. Adabbo, and R. J. J. Williams, *J. Appl. Polym. Sci.*, **29**, 2481 (1984).
19. C. C. Riccardi and R. J. J. Williams, *J. Appl. Polym. Sci.*, **32**, 3445–3456 (1986).
20. B. A. Rozenberg, *Adv. Polym. Sci.*, **75**, 113 (1985).
21. K. Dusek, *Adv. Polym. Sci.*, **78**, 1 (1986).
22. R. B. Prime, in *Thermal Characterization of Polymeric Materials*, E. A. Turi, Ed., Academic Press, New York, 1981, p. 435.
23. B. Carnahan, H. A. Luther, and J. O. Wilkes, *Applied Numerical Methods*, Wiley, New York, 1969.
24. G. Wisanrakkit and J. K. Gillham, *Amer. Chem. Soc. Preprints Div. Polym. Mat. Sci. Eng.*, **59**, 969 (1988).
25. M. T. Aronhime and J. K. Gillham, *J. Appl. Polym. Sci.*, **29**, 2017 (1984).
26. H. E. Adabbo and R. J. J. Williams, *J. Appl. Polym. Sci.*, **27**, 1327–1334 (1982).
27. A. T. DiBenedetto, in L. E. Nielsen, *J. Macromol. Sci. Rev. Macromol. Chem.* C**3**, 69–103 (1969).
28. G. Wisanrakkit and J. K. Gillham, *Am. Chem. Soc. Prepr. Div. Polym. Chem.*, **31** 293 (1990).

Received October 31, 1989
Accepted November 7, 1989